Journal of Alloys and Compounds 508 (2010) 475–479

Contents lists available at ScienceDirect

Journal of Alloys and Compounds

journal homepage: www.elsevier.com/locate/jallcom

Preparation and luminescent properties of a novel red emitting phosphor of $Ca_{1-2x}M_xIn_2O_4$:xEu^{3+} (M = Li, Na, K) for white LED solid-state lighting

Xiaosong Yan, Wanwan Li*, Kang Sun*

School of Materials Science and Engineering, State Key Lab of Metal Matrix Composites, Shanghai Jiao Tong University, 800 Dongchuan Road, Shanghai 200240, PR China

ARTICLE INFO

Article history:
Received 11 February 2010
Received in revised form 15 August 2010
Accepted 24 August 2010
Available online 19 September 2010

PACS:
42.50.Ex

Keywords:
Phosphor
Luminescence
Solid-state reaction

ABSTRACT

The phosphors of $Ca_{1-2x}M_xIn_2O_4$:xEu^{3+} (M = Li, Na, K) were prepared by solid-state reaction method, which showed the characteristic emissions of Eu^{3+} ($^5D_j \rightarrow {}^7F_{j'}$, j = 0, 1, 2, 3 j' = 0, 1, 2, 3 transitions). The emission located at 618 nm due to the $^5D_0 \rightarrow {}^7F_2$ transition was dominantly observed in the photoluminescence (PL) spectrum, leading to a red emission of the phosphors. The phosphors can be excited efficiently by both 394 nm and 465 nm light. Li^+, Na^+, K^+ ions were doped as charge compensators to enhance red emission of the phosphors, and different effects of the alkali metal ions on the luminescence of the phosphors were investigated.

1. 1.Introduction

Solid-state white light-emitting diode (w-LED) is an attractive replacement for the current illumination applications because of its longer service lifetime, lower thermal resistance, more compact size and higher efficiency [1]. The devices combining a yellow emitting YAG:Ce phosphor with a blue emitting InGaN LED chip have been widely commercialized since 1997. However, this type of white light has a less satisfactory color rendering (CRI ~ 70) for the deficiency of color in red and green regions [2]. One of the most promising approaches to solve the problem is the utilization of a near-UV-LED chip (360–410 nm) in combination with blue, green and red emitting phosphors, which provides a more balanced white emission spectrum and a higher color rendering. Presently, the main commercial red phosphor for near-UV-LED is Y_2O_2S:Eu^{3+} [3–4]. However, the sulfide red phosphor is chemically unstable and the absorption efficiency in the near-UV-region is not desirable compared to that of the blue ($BaMgAl_{10}O_{17}$:Eu^{2+}) [5,6] and the green (ZnS:(Cu^+, Al^{3+})) [7] phosphors. Therefore, more attention has been paid to the investigation of the red emitting materials using near-UV-LED as the excitation source in the past few years [8–11], and it is significant to develop new stable phosphors that emit a more intense component in the red region.

Materials containing Eu^{3+} (f^6) fluoresce via transitions from a $^5D_0$ to $^7F_2$ level at 611 nm when Eu^{3+} presents in a non-centrosymmetric site and form useful red phosphors. This approach has been successfully utilized in molybdate and tungstate scheelites [12–15]. However, the emission is composed of only several red sharp lines in lack of light in orange–yellow regions. Oxide semiconductors have been shown to be promising phosphor materials due to their wide band gap, low absorbance in the visible region and their chemical and thermal stabilities [16–21]. Among the oxides, $M'In_2O_4$ (M′ = Ca, Sr) has been widely used as an excellent host material for rare earth metal ions doped phosphors. Tb^{3+} doped $M'In_2O_4$ (M′ = Ca, Sr) was reported to emit green luminescence [19] and the red emitting material of $SrIn_2O_4$:Eu^{3+} was reported to have not only a broad and intense charge transfer band in UV-region but also the intense excitation of Eu^{3+} at around 395 nm and 465 nm which perfectly matches with the emission spectra of both near-UV and blue-LEDs chips [20,21]. However, the radius of Eu^{3+} is 107 pm, which is highly different from that of In^{3+} (80 pm). Therefore, a part of Eu^{3+} ions will be assumed to substitute Sr^{2+} (126 pm) [22]. The difference between the radii of the two types of ions indicates a distortion in the crystal structure when Eu^{3+} is doped to substitute the position of Sr^{2+}, which may lead to a negative influence on the luminescence of the phosphor. Therefore, we have specifically been interested in Eu^{3+} doped $CaIn_2O_4$ because of the similar radius of Ca^{2+} (112 pm) to that of Eu^{3+}. Recently, the white light emission from Eu^{3+} in the $CaIn_2O_4$ host under the excitation of 397 nm light has been reported by Liu and co-workers [23,24]. The white light consists of emission lines from transitions of $^5D_{0,1,2,3}$ excited states

* Corresponding authors.
E-mail addresses: wwli@sjtu.edu.cn (W. Li), ksun@sjtu.edu.cn (K. Sun).

0925-8388/$ – see front matter © 2010 Elsevier B.V. All rights reserved.
doi:10.1016/j.jallcom.2010.08.096

Table 1
Calculated lattice parameters of Eu^{3+} doped $CaIn_2O_4$.

	a (Å)	b (Å)	c (Å)
$CaIn_2O_4$	9.6500	11.3000	3.2100
$CaIn_2O_4$:0.05Eu^{3+}	9.6492	11.3018	3.2106
$CaIn_2O_4$:0.08Eu^{3+}	9.6513	11.3013	3.2122
$CaIn_2O_4$:0.1Eu^{3+}	9.6527	11.2993	3.2141
$CaIn_2O_4$:0.15Eu^{3+}	9.6533	11.2982	3.2154

to the ^7F_j ground states of Eu^{3+}, and is realized at the low doping concentration of Eu^{3+} (~1%). Red emission from $CaIn_2O_4$ doped with a high concentration of Eu^{3+} (up to 10%) was also reported by Liu and co-workers [23], however, to our knowledge, few report about the charge balance in the host lattice of $CaIn_2O_4$ doped with a high concentration of Eu^{3+} (over 5%) for red phosphor can be found.

In this paper, a novel red phosphor $Ca_{1-2x}M_xIn_2O_4$:xEu^{3+} (M = Li, Na, K) with strong luminescence has been prepared. Eu^{3+} is doped in $CaIn_2O_4$ host lattice to obtain a red emitting phosphor, and alkali metal ions such as Li^+, Na^+, K^+ are co-doped as charge compensators to enhance the luminescence of the Eu^{3+} doped $CaIn_2O_4$. The effects of the charge compensation on the luminescent properties of different alkali metal ions are investigated. The performance of our phosphors is also compared to some popular red phosphors of Y_2O_2S:Eu^{3+} and $CaMoO_4$:Eu^{3+}.

2. Experimental

A series of Eu^{3+} doped and Eu^{3+}, M^+ (M = Li, Na, K) co-doped $CaIn_2O_4$ phosphors were prepared by traditional solid-state reactions. The starting materials $CaCO_3$(A.R), In_2O_3(A.R) and Eu_2O_3(4N) were weighted with an appropriate stoichiometric ratio. The molar concentration of the activator Eu^{3+} ions varied from 5% to 18%. An appropriate amount of Li_2CO_3(A.R), Na_2CO_3(A.R) and K_2CO_3(A.R) were added as the charge compensators. All the starting powders were blended and grinded by ball milling thoroughly at 300 rpm for 3 h. After dried at 80 °C for 12 h, the homogeneous mixture obtained was put into an alumina crucible and calcined in a muffle furnace at the temperature of 900 °C for 3 h into the intentional sample.

The synthesized samples were identified by X-ray diffraction (XRD), which was recorded on a BRUKER-AXS X-ray diffraction running Cu Kαradiation at 40 kV and 250 mA. The measurements of photoluminescence (PL) and photoluminescence excitation (PLE) spectra were performed by using a SHIMADZU RF-2550 spectrometer equipped with a 150 W xenon lamp under a working voltage of 400 V. The excitation and emission slits were set at 5.0 nm. The CIE chromaticity coordinates were measured by using a SPR 920F scanning spectroradiometer. All the measurements were performed at room temperature.

3. Results and discussion

3.1. Structure of Eu^{3+} doped and Eu^{3+}, M^+ (M = Li, Na, K) co-doped $CaIn_2O_4$

The XRD patterns of Eu^{3+} doped $CaIn_2O_4$ samples are shown in Fig. 1, and the samples are synthesized without any charge compensation. According to JCPDS card 17-0643, $CaIn_2O_4$ has an orthorhombic crystal structure with the P$ca2_1$ or Pbcm space group, and its lattice parameter is a = 9.650 Å, b = 11.300 Å, c = 3.210 Å. $CaIn_2O_4$ has two kinds of InO_6 octahedra. InO_6 octahedra are connected to each other by sharing edges structure, while Ca is located in the tunnel. When the concentration of Eu^{3+} is below 0.18, the XRD patterns of the samples are consistent with the standard data of $CaIn_2O_4$. The calculated lattice parameters of Eu^{3+} doped $CaIn_2O_4$ are listed in Table 1 and little variation is found in all the three lattice parameters with the increasing concentration of Eu^{3+}. The ionic radius of Eu^{3+} is 107 pm, which is similar to that of Ca^{2+} (112 pm), and larger than that of In^{3+} (80 pm). Thus, Eu^{3+} is expected to occupy the Ca^{2+} site in the host lattice [23]. However, the diffraction peaks of In_2O_3 and $EuInO_3$ are found when the concentration of Eu^{3+} is 0.18. With a high Eu^{3+} doping concentration in $CaIn_2O_4$, it may be difficult for the Eu^{3+} ions to be fully introduced into Ca sites in order to keep charge balanced. Thus In_2O_3 and $EuInO_3$ generate as the impurity phase.

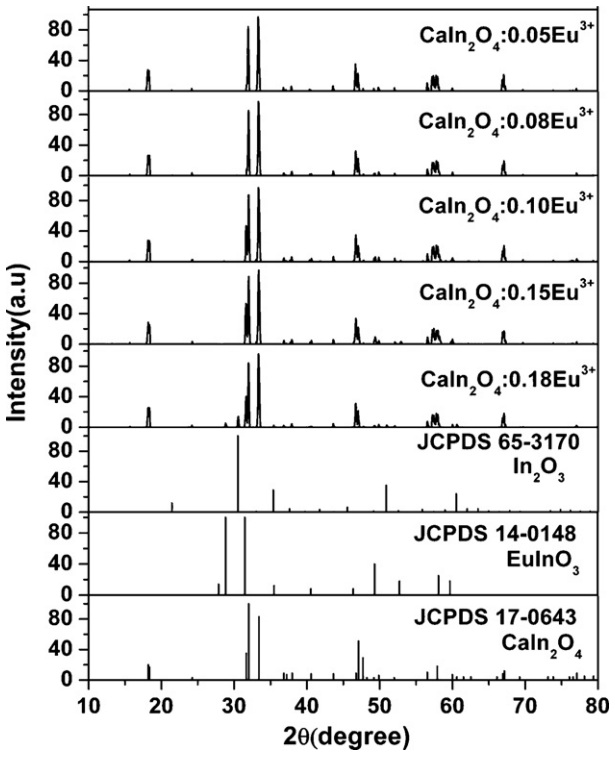

Fig. 1. XRD patterns of Eu^{3+} doped $CaIn_2O_4$, with the standard data of $CaIn_2O_4$ (JCPDS No.17-0643), In_2O_3 (JCPDS No.65-3170), $EuInO_3$ (JCPDS No.14-0148).

The XRD patterns of Eu^{3+}, M^+ (M = Li, Na, K) co-doped $CaIn_2O_4$ samples are shown in Fig. 2. Due to the different valence states with In^{3+}, alkali metal ions are also expected to substitute for the Ca^{2+} sites rather than the In^{3+} sites, and the charge loss of the host lattice compensated by the co-doped alkali metal ions of M^+ can be described by

$$2Ca^{2+} \rightarrow Eu^{3+} + M^+$$

The powder X-ray diffraction results show that all the patterns of the samples are consistent with the standard data of $CaIn_2O_4$, which indicates that the co-doped Eu^{3+} ions and Li^+, Na^+, K^+ ions did

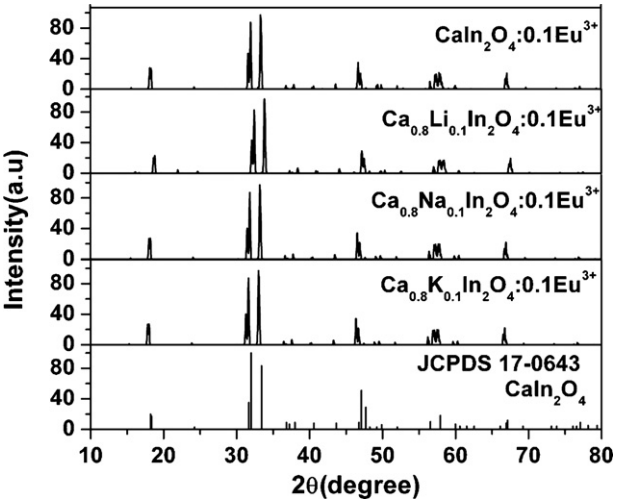

Fig. 2. XRD patterns of Eu^{3+} M^+ (M = Li, Na, K) co-doped $CaIn_2O_4$, with the standard data of $CaIn_2O_4$ (JCPDS No.17-0643).

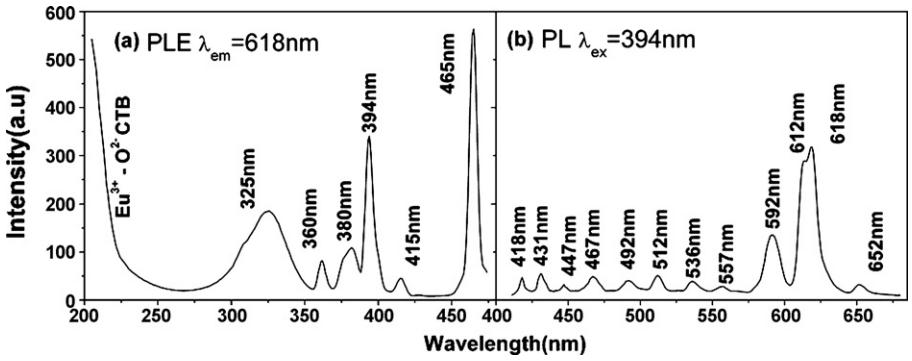

Fig. 3. PLE (a) and PL (b) spectra of $CaIn_2O_4$:0.05Eu^{3+} sample with λ_{ex} = 394 nm and λ_{em} = 618 nm.

not cause significant changes in the host lattice structure. With Na^+ and K^+ as additives, the diffraction peaks shift to a smaller angle, but the doping Li^+ ions in $CaIn_2O_4$:Eu^{3+} results in the diffraction peaks shifting to a larger angle. These shifts of the XRD peaks are attributed to the substitution of the Ca^{2+} ions by alkali metal ions in host lattice [25]. The radii of K^+ (138 pm) and Na^+ (118 pm) are larger than that of Ca^{2+} (112 pm), which results in a smaller angle shift of the peaks in the XRD patterns. Accordingly, the radius of Li^+ (92 pm) is smaller than that of Ca^{2+}, which leads to a larger angle shift of the diffraction peaks [26].

3.2. Luminescent properties of Eu^{3+} doped $CaIn_2O_4$

Fig. 3 shows the PLE (a) and PL (b) spectra of $CaIn_2O_4$:0.05Eu^{3+}. The PL spectrum of $CaIn_2O_4$:0.05Eu^{3+} is composed of several sharp lines, which can be attributed to the characteristic emissions of Eu^{3+} ions. The strongest red emission at around 612 nm and 618 nm is owing to the hypersensitive $^5D_0 \rightarrow {}^7F_2$ transition of Eu^{3+} forced by an electric dipole mechanism, and the weaker emission located at 592 nm is due to the $^5D_0 \rightarrow {}^7F_1$ magnetic dipole transition of Eu^{3+}, which is reported to be insensitive to the site symmetry [14]. The emission here indicates a lack of inversion symmetry at the Eu^{3+} sites in $CaIn_2O_4$:Eu^{3+} and the break of parity selection rules. The other features of the PL spectrum are the sharp emission lines originated within the intra-shell transitions from the $^5D_{0,1,2,3}$ excited levels to the ^7F_j ground states of Eu^{3+}, such as $^5D_3 \rightarrow {}^7F_1$(418 nm), $^5D_3 \rightarrow {}^7F_2$(431 nm), $^5D_3 \rightarrow {}^7F_3$(447 nm), $^5D_2 \rightarrow {}^7F_0$(467 nm), $^5D_2 \rightarrow {}^7F_2$ (492 nm), $^5D_2 \rightarrow {}^7F_3$ (512 nm), $^5D_1 \rightarrow {}^7F_1$ (537 nm), $^5D_1 \rightarrow {}^7F_2$ (557 nm), $^5D_0 \rightarrow {}^7F_3$ (652 nm)[23]. Although many types of emissions from $^5D_{0,1,2,3}$ excited states of Eu^{3+} have been observed, the transition of $^5D_0 \rightarrow {}^7F_2$ is dominantly observed in the PL spectrum, leading to a red emission color of the sample.

The PLE spectrum of $CaIn_2O_4$:0.05Eu^{3+} consists of broad excitations band from 205 nm to 350 nm and some sharp lines beyond 350 nm. The broad excitation band below 270 nm is due to the charge transfer transition between O^{2-} and Eu^{3+} [23]. $CaIn_2O_4$ semiconductor was reported to have a band gap value of 3.9 eV (321 nm) [27], which is basically consistent with the weak broad band peak at 325 nm, thus the excitation band extending to 325 nm is attributed to the band gap of the $CaIn_2O_4$ host lattice. Beyond 350 nm, the sharp excitation lines at longer wavelengths correspond to the characteristic f–f transitions absorption of Eu^{3+}. The lines in the spectrum can be assigned to $^7F_0 \rightarrow {}^5D_4$ (360 nm), $^7F_0 \rightarrow {}^5G_4$ (380 nm), $^7F_0 \rightarrow {}^5L_6$ (394 nm), $^7F_1 \rightarrow {}^5D_3$ (415 nm), $^7F_0 \rightarrow {}^5D_2$ (465 nm). The main excitation lines are $^7F_0 \rightarrow {}^5L_6$ (394 nm) and $^7F_0 \rightarrow {}^5D_2$ (465 nm), which means this phosphor is well matched with the emission wavelengths of both near-UV-LEDs and blue-LEDs.

The photoluminescence of $CaIn_2O_4$ with different concentrations of the doping Eu^{3+} is investigated to obtain the favorable molar doping Eu^{3+} concentration. Fig. 4 shows the dependence of relative intensities of the red emission peaks of $CaIn_2O_4$:xEu^{3+} phosphors on the concentrations of Eu^{3+}. Generally, an increase in the activator concentration increases the energy stored by the ions, which will enhance the emission intensity of the transitions of activator ions [14]. However, Eu^{3+} ions are difficult to be fully introduced to the host lattice when a high concentration of Eu^{3+} is doped in $CaIn_2O_4$ due to the charge balance, and both defects and impurity phase generate as shown in the XRD patterns. Thus, the probability that the optical excited electrons trapped in defects or impurity sites increases [14], which will result in a decrease of the emission intensity. Consequently, there is an optimum concentration of activator ions, and the favorable molar concentration of Eu^{3+} in $CaIn_2O_4$:xEu^{3+} in our experiments is 15%, as shown in Fig. 4.

3.3. Luminescent properties of Eu^{3+}, M^+ (M = Li, Na, K) co-doped $CaIn_2O_4$

In order to make Eu^{3+} fully introduced into the Ca^{2+} sites, the alkali metal ions are used to substitute some of the Ca^{2+} ions to make the charge compensation. The PL spectra of $Ca_{0.7}M_{0.15}In_2O_4$:0.15Eu^{3+} (M = Li, Na, and K) and $CaIn_2O_4$:0.15Eu^{3+} recorded under the same experimental conditions are shown in Fig. 5. The as-prepared $Ca_{0.7}Na_{0.15}In_2O_4$:0.15Eu^{3+} shows the highest emission intensity of $^5D_0 \rightarrow {}^7F_2$ transition among the phosphors, which is about 1.93 times as intense as that of $CaIn_2O_4$:0.15Eu^{3+}. The as-prepared $Ca_{0.7}K_{0.15}In_2O_4$:0.15Eu^{3+} and

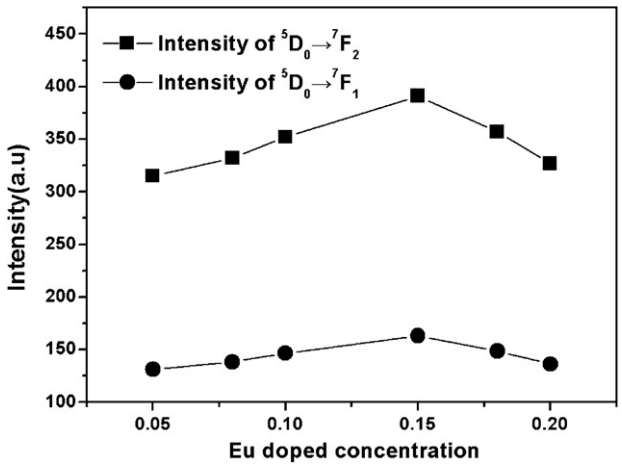

Fig. 4. The dependence of red emission intensity on Eu^{3+} concentration (x) in $CaIn_2O_4$:xEu^{3+} with λ_{ex} = 394 nm.

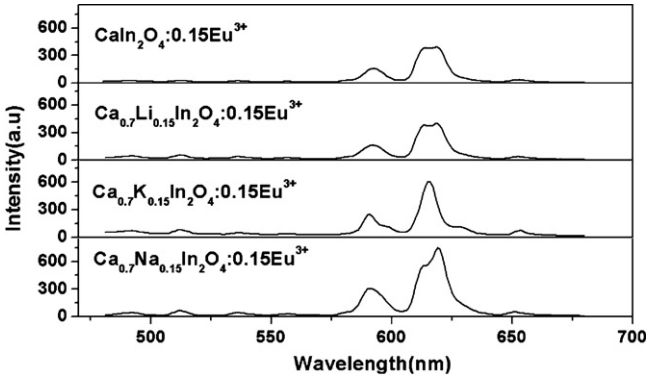

Fig. 5. The PL spectra of $Ca_{0.7}M_{0.15}In_2O_4$:0.15Eu^{3+} (M = Li, Na, K) and $CaIn_2O_4$:0.15Eu^{3+} samples with λ_{ex} = 394 nm.

$Ca_{0.7}Li_{0.15}In_2O_4$:0.15Eu^{3+} also show about 1.57 times and 1.02 times as intense as that of $CaIn_2O_4$:0.15Eu^{3+} respectively. The enhancement of PL intensity can be attributed to the result of charge compensation. Obviously, the appropriate doping of alkali metal ions in $CaIn_2O_4$:Eu^{3+} phosphor can effectively enhance the red emission.

The dependence of the red emission intensities located at 618 nm on Eu^{3+} concentrations (x) in $CaIn_2O_4$:xEu^{3+} and $Ca_{1-2x}M_xIn_2O_4$:xEu^{3+} (M = Li, Na, and K) is shown in Fig. 6. All the three types of alkali metal ions are able to enhance the luminescence of the phosphors, and the phosphors co-doped with Na$^+$ ions show the highest red emission intensities. The radius of Na$^+$ is 118 pm, which is similar to that of Ca^{2+} (112 pm), while the radius of Li$^+$ is 92 pm and the radius of K$^+$ is 138 pm. Thus Na$^+$ is expected to cause less distortion in the crystal structure of the phosphors. Moreover, the enhancement of the emission intensity is very limited with a low concentration of Eu^{3+}, which can be assigned to the fact that less charge imbalance forms during the substitution of Ca^{2+} by Eu^{3+} when the concentration of Eu^{3+} is low, and the effect of the charge compensators is limited.

3.4. Comparison of luminescent properties of Eu^{3+}, M^+ (M = Li, Na, K) co-doped $CaIn_2O_4$ with Y_2O_2S:Eu and $CaMoO_4$:Eu

Y_2O_2S:Eu^{3+} and $CaMoO_4$:Eu^{3+} are reported to be good red phosphors for the solid-state lighting, and a series of samples of both Y_2O_2S:Eu^{3+} and $CaMoO_4$:Eu^{3+} with different concentrations of Eu^{3+} are prepared according to the references of [28] and [14] respectively. The molar doping concentrations of Eu^{3+} to obtain the highest emission intensities are 0.05 and 0.2 for Y_2O_2S and $CaMoO_4$ respectively, which are very close to the results reported by Reddy et al. [28] and Hu et al. [14], thus the samples of Y_2O_2S:0.05Eu^{3+} and $CaMoO_4$:0.2Eu^{3+} are selected to compare with our phosphors. The phosphors are washed and sieved, and the particle size distribution patterns of the phosphors are shown in Fig. 7. All the phosphors present a narrow particle size distribution, and the average particle sizes of the phosphors are similar. The PL spectra of Y_2O_2S:0.05Eu^{3+}, $CaMoO_4$:0.2Eu^{3+} and $Ca_{0.7}Na_{0.15}In_2O_4$:0.15Eu^{3+} under the excitation wavelength of 394 nm are shown in Fig. 8. The CIE chromaticity coordinates and the relative emission intensities of some phosphors under the excitation wavelength of 394 nm are listed in Table 2. The red emission intensity of Y_2O_2S:0.05Eu^{3+} is lower than that of $CaIn_2O_4$:xEu^{3+} and $Ca_{1-2x}M_xIn_2O_4$:xEu^{3+} (M = Li, Na, and K) phosphors, and shows only 42% as that of the $Ca_{0.7}Na_{0.15}In_2O_4$:0.15Eu^{3+}. The emission intensity of $CaMoO_4$:0.2Eu^{3+} shows only 72% as that of $Ca_{0.7}Na_{0.15}In_2O_4$:0.15Eu^{3+}. As shown in Fig. 9, the CIE chromatic-

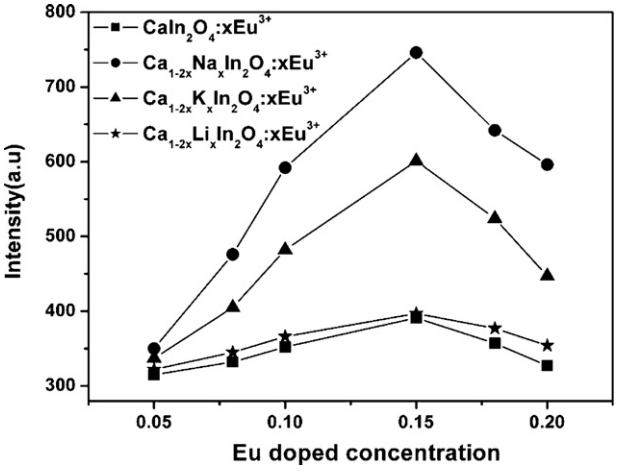

Fig. 6. The dependence of red emission intensity located at 618 nm on Eu^{3+} concentrations (x) in $CaIn_2O_4$:xEu^{3+} and $Ca_{1-2x}M_xIn_2O_4$:xEu^{3+} (M = Li, Na, K) with λ_{ex} = 394 nm.

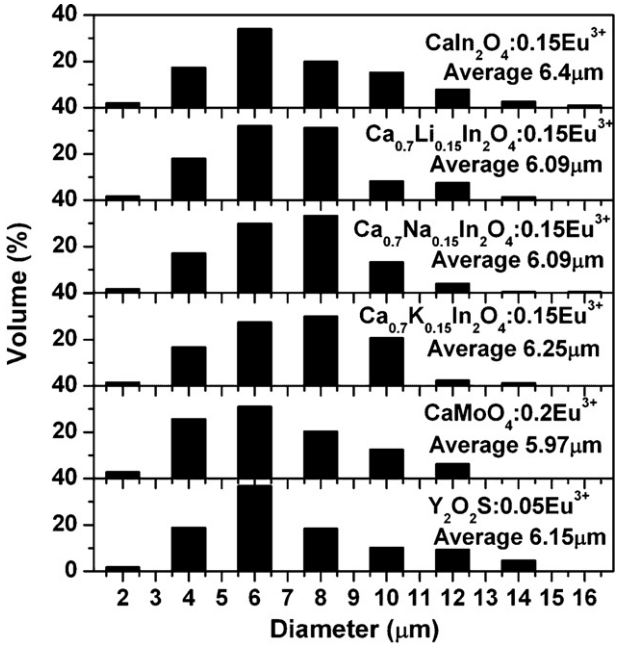

Fig. 7. Particle size distribution patterns of $CaIn_2O_4$:0.15Eu^{3+}, $Ca_{0.7}M_{0.15}In_2O_4$:0.15Eu^{3+}, Y_2O_2S:0.05Eu^{3+} and $CaMoO_4$:0.2 Eu^{3+}.

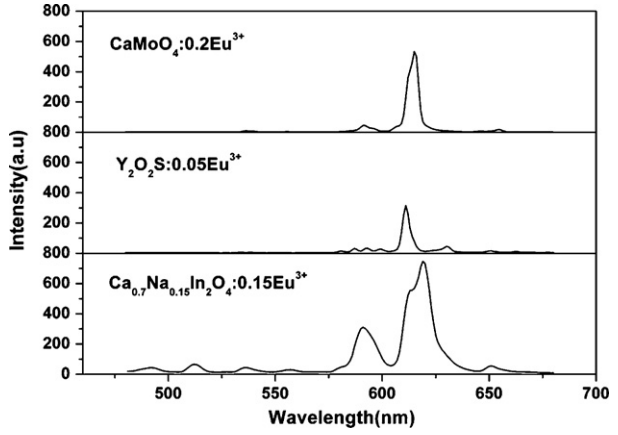

Fig. 8. The PL spectra of Y_2O_2S:0.05Eu^{3+}, $CaMoO_4$:0.2 Eu^{3+} and $Ca_{0.7}Na_{0.15}In_2O_4$:0.15Eu^{3+} samples with λ_{ex} = 394 nm.

Table 2
The CIE chromaticity coordinates and the $^5D_0 \rightarrow {}^7F_2$ relative intensity of the phosphors under the excitation wavelength of 394 nm.

Phosphor	CIE chromaticity coordinates		$^5D_0 \rightarrow {}^7F_2$ relative intensity
	x	y	
$CaIn_2O_4$:0.15Eu^{3+}	0.63	0.35	1.21
$Ca_{0.7}Na_{0.15}In_2O_4$:0.15Eu^{3+}	0.63	0.34	2.34
$Ca_{0.7}K_{0.15}In_2O_4$:0.15Eu^{3+}	0.63	0.35	1.91
$Ca_{0.7}Li_{0.15}In_2O_4$:0.15Eu^{3+}	0.63	0.34	1.23
Y_2O_2S:0.05Eu^{3+}	0.61	0.34	1
$CaMoO_4$:0.2Eu^{3+}	0.61	0.32	1.71

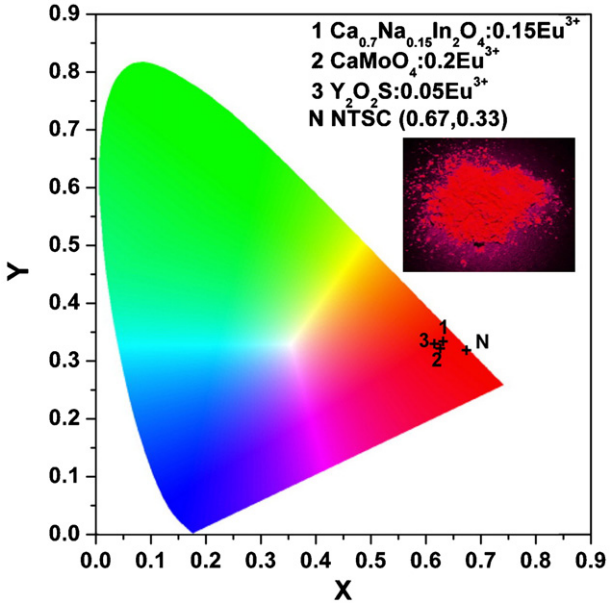

Fig. 9. CIE x, y chromaticity diagram showing the color of $Ca_{1-2x}M_xIn_2O_4$:xEu^{3+} as compared to the Y_2O_2S:0.05Eu^{3+} and $CaMoO_4$:0.2Eu^{3+} phosphors. Inset shows a photograph for one of the $Ca_{1-2x}M_xIn_2O_4$:xEu^{3+} red phosphors on excitation wavelength of 394 nm.

ity coordinates of all the samples indicate that the CIE chromaticity coordinates of $Ca_{1-2x}M_xIn_2O_4$:xEu^{3+} are closer to the standard of National Television Standard Committee (NTSC) (0.67, 0.33) than those of the other two phosphors. Obviously, the novel phosphor of $Ca_{1-2x}M_xIn_2O_4$:xEu^{3+} (M = Li, Na, K) is an efficient red emitting phosphor for light-emitting diodes applications.

4. Conclusions

Luminescent powders of $CaIn_2O_4$:xEu^{3+} and $Ca_{1-2x}M_xIn_2O_4$:xEu^{3+} have been successfully synthesized by solid-state reactions. The phosphors can be efficiently excited by light with wavelengths of 394 nm and 465 nm, which are well matched with the emission wavelengths of both near-UV-LEDs and blue-LEDs. Under the excitation of near-UV light, the phosphors show strong red emission lines corresponding to the characteristic emissions of Eu^{3+} ($^5D_j \rightarrow {}^7F_{j'}$, j = 0, 1, 2, 3 j' = 0, 1, 2, 3 transitions), and the emission located at 618 nm due to the forced electric dipole $^5D_0 \rightarrow {}^7F_2$ transition is dominantly observed in the PL spectrum. Ions of Na^+, K^+ and Li^+ have been doped in the host lattice as charge compensators to keep the charge balance. All the three types of alkali metal ions result in an enhanced intensity of the luminescence of the Eu^{3+} doped $CaIn_2O_4$, and Na^+ is demonstrated to be the best one due to its similar ion radius to Ca^{2+}. $Ca_{0.7}Na_{0.15}In_2O_4$:0.15Eu^{3+} shows much stronger emission intensity than that of Y_2O_2S:0.05Eu^{3+} and $CaMoO_4$:0.2Eu^{3+}, which indicates $Ca_{1-2x}M_xIn_2O_4$:xEu^{3+} is a promising red emitting phosphor for the white LED solid-state lighting.

Acknowledgments

This work was financially supported by National Natural Science Foundation of China (Project No. 50902093). We thank Instrumental Analysis Center of SJTU for the assistance with XRD characterization. We also thank Shanghai Sunny New Technology Development Co., Ltd. for their support.

References

[1] E.F. Schubert, J.K. Kim, Science 308 (2005) 1274–1278.
[2] T. Gessmann, E.F. Schubert, J. Appl. Phys. 95 (2004) 2203–2216.
[3] D.V. Ligia, B.S. Elizabeth, D.R. Marian, J. Mater. Chem. 7 (1999) 2113–2116.
[4] J. Dhanaraj, R. Jagannathan, D.C. Trivedi, J. Mater. Chem. 13 (2003) 1778–1782.
[5] Z.S. Wu, Y. Dong, J.Q. Jiang, J. Alloys Compd. 467 (2009) 605–610.
[6] Z. Chen, Y.W. Yan, J.M. Liu, Y. Yin, H.M. Wen, J.Q. Zao, D.H. Liu, H.M. Tian, C.S. Zhang, S.D. Li, J. Alloys Compd. 473 (2009) L13–L16.
[7] C.C. Kao, Y.C. Liu, Mater. Chem. Phys. 115 (2009) 463–466.
[8] L.H. Yi, X.P. He, L.Y. Zhou, F.Z. Gong, R.F. Wang, J.H. Sun, J. Lumin. 130 (2010) 1113–1117.
[9] A. Xie, X.M. Yuan, F.X. Wang, Y. Shi, J. Li, L. Liu, Z.F. Mu, J. Alloys Compd. 501 (2010) 124–129.
[10] H.Y. Du, J.F. Sun, Z.G. Xia, J.Y. Sun, J. Electrochem. Soc. 156 (2009) J361–J366.
[11] L.Y. Zhou, J.L. Huang, F.Z. Gong, Y.W. Lan, Z.F. Tong, J.H. Sun, J. Alloys Compd. 495 (2010) 268–271.
[12] M.D.M. Haque, H.I. Lee, D.K. Kim, J. Alloys Compd. 481 (2009) 792–796.
[13] F. Lei, B. Yan, H.H. Chen, J.T. Zhao, J. Am. Ceram. Soc. 92 (2009) 1262–1267.
[14] Y.S. Hu, W.D. Zhuang, H.Q. Ye, D.H. Wang, S.S. Zhang, X.W. Huang, J. Alloys Compd. 390 (2005) 226–229.
[15] F.Q. Ren, D.H. Chen, J. Alloys Compd. 499 (2010) 53–56.
[16] Z.D. Hao, J.H. Zhang, X. Zhang, X.Y. Sun, Y.S. Luo, S.Z. Lu, Appl. Phys. Lett. 90 (2007) 261113.
[17] Z.Y. Hou, P.P. Yang, C.X. Li, L.L. Wang, H.Z. Lian, Z.W. Quan, J. Lin, Chem. Mater. 20 (2008) 6686–6696.
[18] X.M. Liu, J. Lin, J. Mater. Chem. 18 (2008) 221–228.
[19] S.P. Khatkar, V.B. Taxak, S.D. Han, J.Y. Park, D. Kumar, Mater. Chem. Phys. 98 (2006) 528–531.
[20] Z.P. Yang, J. Tian, S.L. Wang, G.W. Yang, X. Li, P.L. Li, Mater. Lett. 62 (2008) 1369–1371.
[21] C.E. Rodriguez, N. Perea, G.A. Hirata, S.P. Denbaars, J. Phys. D: Appl. Phys. 41 (2008) 092005.
[22] A. Baszczuk, M. Jasiorski, M. Nyk, J. Hanuza, M. Maczka, W. Strek, J. Alloys Compd. 394 (2005) 88–92.
[23] X.M. Liu, C.X. Li, Z.W. Quan, Z.Y. Cheng, J. Lin, J. Phys. Chem. C 111 (2007) 16601–16607.
[24] X.M. Liu, C.K. Li, J. Lin, Appl. Phys. Lett. 90 (2007) 081904.
[25] J. Liu, H.Z. Lian, C.S. Shi, Opt. Mater. 29 (2007) 1591–1594.
[26] Y.S. Lin, R.S. Liu, B.M. Cheng, J. Electrochem. Soc. 152 (2005) J41–J45.
[27] G. Blasse, B. Grabmaier, B. C. Luminescence. Materials; Springer-Verlag: Berlin, 1994; Chapter 4–5.
[28] K.R. Reddy, K. Annapurna, S. Buddhudu, Mater. Res. Bull. 31 (1996) 1355–1359.